

INFLUENCE OF SHOT PEENED ALUMINIUM ALLOY 7075-T651 ON FATIGUE AND CORROSION RESISTANCE¹

U. Zupanc²
J. Grum³

Abstract

Shot peening (SP) is an important and well-known cold working process having been used in industrial applications for a long time. Shot peening as intense plastic deformation in the thin surface layer affects cold surface hardening by primary inducing favourable residual compressive stresses. It is used in order to increase fatigue strength in operation and to improve corrosion resistance of treated material. Pitting corrosion has a major influence on aging of structural elements made of high-strength aluminium alloys as corrosion pits lead to much earlier fatigue crack initiation under tensile dynamic loading. The paper deals with surface integrity of shot peened high-strength 7075-T651 aluminium alloy. The paper describes effects of SP treatment by presenting analyses of surface roughness measurement, residual stresses, material bending fatigue resistance, fractographic analysis of fatigued samples and electrochemical potentiodynamic testing.

Keywords: Aluminium alloys; Pitting corrosion; Fatigue crack initiation.

¹ Technical contribution to the 18th IFHTSE Congress - International Federation for Heat Treatment and Surface Engineering, 2010 July 26-30th, Rio de Janeiro, RJ, Brazil.

² Welding Institute, Ptujška 19, SI-1000 Ljubljana, Slovenia. E-mail: uros.zupanc@i-var.si. Tel: (00) 386 1 2809 422; Fax: (00) 386 1 2809 442.

³ University of Ljubljana, Faculty of Mechanical Engineering, Aškerčeva 6, SI-1000 Ljubljana. E-mail: janez.grum@fs.uni-lj.si.

1 INTRODUCTION

Pitting corrosion has a major influence on aging of structural elements made of high-strength aluminium alloys. Aluminium alloy 7075 in alloy system Al-Zn-Mg-Cu contains a high number of intermetallic particles, i.e. constituent particles, where heterogeneity of a microstructure has an essential influence on corrosion properties.^[1] Due to electrochemical reactions in a corrosive environment, dissolved (pit) areas lead to earlier fatigue crack initiation. Numerous studies relate corrosion pits to reduced material strength under dynamic loading.^[2-4] The depth of corrosion pits on fatigued material is the most important affecting factor. With longer exposure to a corrosive environment the pit depth increases. On the basis of microscopic analyses measured, a critical pit depth to initiate fatigue crack measured between 40 and 60µm.^[5-6] A cause of fatigue crack initiation under dynamic loading in a corrosive medium is a stress concentration at pit locations. Stress levels at a pit area are in the magnitude of material plane strain fracture toughness, from which it is possible to estimate fatigue crack initiation.^[7-8] In order to improve material resistance to corrosion fatigue it is necessary to reduce pit-tip stresses in the corroded pits areas. Shot peening (SP) as intense plastic deformation in a thin surface layer affects fatigue properties by inducing favourable residual compressive stresses. Studies of SP-treated specimens prove increased material resistance to crack initiation, which increases fatigue life by a factor of 1.2 to 6.^[9-12] To assure appropriate surface properties, control and optimization of SP parameters is essential as reported in.^[13-14]

The present investigation has been made as part of an ongoing study into the effects of SP treatment. A series of tests were performed to analyse the effects of SP treatment on surface pitting corrosion properties. The objective of the present study was to investigate the influence of surface hardening by SP treatment on electrochemical stability and corrosion fatigue properties of high strength aluminium alloy 7075-T651 in 5% NaCl salt fog conditions. Induced residual compressive stresses retard fatigue crack initiation so better corrosion fatigue properties of SP treated specimens in salt fog chamber were expected. Electrochemical potentiodynamic testing in chloride solution supported by using Tafel analysis was conducted to investigate the effect of SP on corrosion characteristics.

2 EXPERIMENTAL DETAILS

For the experiment a rolled plate of high-strength aluminium alloy 7075-T651 of 20mm in thickness was delivered with the chemical composition (in wt.%) Al-5.78Zn-2.56Mg-1.62Cu-0.21Cr-0.05Mn-0.04Ti-0.09Si-0.18Fe and tested mechanical properties: Rm=585MPa, Rp02=532MPa and A50=12%. Hourglass-shaped specimens of fatigue testing were cut out of the delivered plate in a direction perpendicular to the direction of rolling (Fig. 1). In research the prepared specimens were evaluated in four different research combinations: (a) as-machined (AM); (b) as-machined and corroded (AM & Corr); (c) shot-peened (SP); (d) shot-peened and corroded (SP & Corr). The specimens were SP-treated from all sides at the Metal Improvement Company in Germany using an air-blast machine. Steel shot MI-170 with hardness ranging between 55 and 65 HRC and nominal diameter 0.40mm was chosen for the purpose. In order to avoid medium collision, the angle of nozzle inclination was shifted by 5° with regard to the vertical axis. With all the specimens treated a constant specimen distance from the nozzle of around 120mm was

maintained. With experiment surface coverage set to 150% comparative Almen intensity value of 12A was achieved.

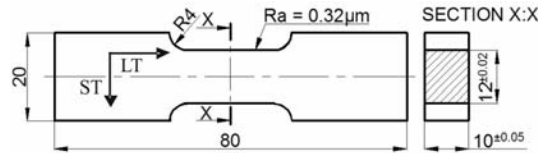


Figure 1. Fatigue specimen details and dimensions (in mm).

Prepared specimens were placed for 168 hours (7days) in a 5% NaCl solution fog chamber for corrosion resistance testing in accordance with ASTM B117.^[15] Before the corrosion process, the SP-treated specimens were cleaned with concentrated HNO₃ acid to avoid surface contamination by possible steel shot residues at the specimen surface. The prepared solution had a pH value of 6.5. Specimens were placed individually parallel to each other on plastic supports at an angle of 20° with regard to a vertical axis. In order to provide uniform exposure of the surface to pitting corrosion, the specimens were being turned every 24 hours during testing. After the exposure of the specimens in the salt fog chamber corrosive pits were covered with corrosion products at the specimen surfaces, particularly with an amorphous gelatinous white gel Al(OH)₃. For the analysis of surface roughness and assessment of the pit size at the surface, the corrosion products were removed with hard polymer wire brush in a water-diluted HNO₃ acid at room temperature.

The evaluation of tested specimens comprised surface properties and residual-stress measurement in thin hardened layer. Measurement of surface roughness was made with device Taylor Hubson Form Talysurf Series 2. The chosen scanned surface of 1x1mm² in size had a linear spacing of 0.5 μm in X axis, 2 μm in Y axis, and 16nm in Z axis. Residual-stress measurements with a semi destructive hole-drilling method in accordance with ASTM 837^[15] were made using device SINT MTS300 with Restran software and measuring rosettes HBM 1.5/120RY61S. Fatigue testing was carried out without preliminary removal of the corrosion products from the surface. Bending fatigue testing of the specimens was carried out with device Rumul Cracktronic at room temperature. A constant amplitude bending stress was applied in the range of maximum applied stresses between 15 and 65% of delivered material tensile strength R_m. The testing resonant stress frequency was 107Hz using sinusoidal wave form at a stress ratio R=0.05. A criterion of specimen failure was a drop of inherent oscillation by more than 3%, where fatigue cracks occurred in a depth up to 4mm. In the present study a run-out criterion as limit of fatigue strength was set at 10 million cycles. Fractured surfaces of all fatigued specimen were further evaluated using a scanning electron microscope (SEM). Electrochemical potentiodynamic testing was conducted in a 0.1M chloride solution from analytical grade chemical and distilled water with a pH value of 6.5. For electrochemical testing as-machined and SP-treated hourglass specimens were sectioned in the form of discs of 15 mm in diameter in the longitudinal (L) direction, rinsed with distilled water and well dried. A Gamry Potentiostat/Galvanostat PCIII was used. A three-electrode corrosion cell was used, with the working electrode embedded in a teflon holder. The exposed area measured 0.785 cm². A saturated calomel electrode (SCE) served as a reference electrode and two stainless-steel rods as counter electrodes. Following a 1-hour stabilization at open circuit potential (OCP), measurements were performed in the following order: linear polarization, ± 10 mV vs. OCP, using a scan rate of 0.1

mV/s and potentiodynamic curves, starting from – 250 mV vs. OCP up to 1 V using scan rate of 1 mV/s. All potentials are reported with respect to SCE scale.

3 RESULTS AND DISCUSION

The results of surface integrity analysis, residual-stress measurement, fatigue testing with post fatigue fractographic analysis and electrochemical testing are presented in following sections.

3.1 Surface Integrity Analysis

SP treatment and pitting corrosion of tested specimens essentially changed surface roughness. Data on final surface roughness can be used to predict material resistance to fatigue properties as suggested by.^[17] Results of measurement of arithmetic average (Ra) and root mean square (Rq) surface roughness after SP treatment and exposure in the salt chamber are given in Table 1. Reference surface roughness of the as-machined specimens, is a result of grinding with emery paper up to granulation of #1000. As-machined specimens exposed to corrosion in the salt chamber essentially increased by four times, due to the formation of pits.

Table 1. Surface roughness measurement results

Treatment	As-machined	Corroded	Shot-peened	SP+Corroded
Ra (µm)	0.32	1.24	5.81	6.27
Rq (µm)	0.47	2.02	7.09	7.81

The pits were oriented in agreement with local dissolution zones of constituent particle lined up in the rolling direction (Fig. 2). The number of pits at the surface in a depth exceeding 20µm at the surface analyzed of 1x1mm² was ~15. Changes in surface roughness on SP-treated specimens are contributed to local surface plastic deformation from absorbed medium kinetic energy. The diameter of the dimples was ranging between 150-200µm. Due to the formation of corrosion pits, an increase by 10% with regard to the SP treated specimen was observed. The pits formed after SP treatment were not perceptibly oriented with regard to the rolling direction, due to local plastic deformation of the constituent particles in surface layer. The surface was additionally evaluated with the SEM analysis using a secondary electron imaging (SEI) signal at chosen location marked with an arrow. The pit lengths at the as-machined and corroded material measured in length up to 500µm, and width to 10-40µm. Separate local pits combined in longer corrosion lines at the area of local dissolution. The corrosion pits grew not only in the rolling directions but did also coalescent with the pits in the direction perpendicular to rolling.

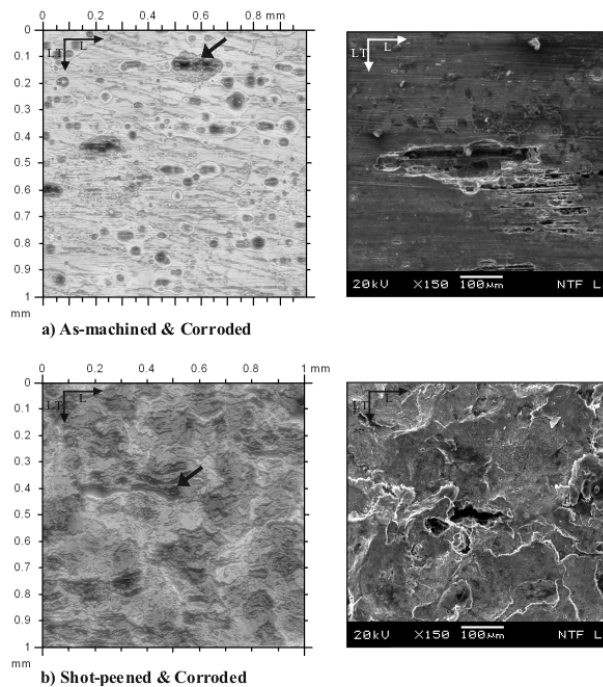


Figure 2. Surface roughness properties of corroded specimens (left) with SEM images (right) at pits marked with arrow.

After SP treatment the number and size of pits at the surface decreased perceptibly. The SP-treated specimens exposed to the corrosive environment contained fewer surface pits, which indicated a favourable influence of the SP treatment on a smaller density of surface pits. Average corrosion pit length at the SP-treated specimens measured in length up to 50-100µm, and their width to 30-50µm. The pit density at the surface of the SP-treated specimens was essentially smaller and amounted to around 5-7 pits per 1mm². The results of our measurements on pit density are comparable to those stated in.^[18-19] Due to surface roughness measuring machine limitations and the fact that pits beneath the surface can be much larger as observed on surface, the true pit widths and depths were evaluated further in the post fatigue fractographic analysis.

3.2 Residual Stresses

Residual stresses measured in the thin hardened surface layer provide information on the depth of cold hardening by SP treatment. Residual stresses are one of key influences on material fatigue resistance, also in corrosive environment. Figure 3 shows measured residual stresses as a function of depth. Prior to SP treatment the as-machined specimens showed residual stresses in the thin surface layer amounting to around -50MPa, induced most probably due to specimen preparation. Residual compressive stresses after SP treatment amounted to around -320MPa, i.e. to around 55% Rm of the delivered material. Depths up to 500µm of the induced residual stresses after SP treatment are greater than the depth of typical corrosion pits; therefore, residual stresses should influence on local stress concentrations at pit area in fatigue testing. Further, the study of residual stress measurements showed the surface pits at local dissolution zones can result in a relief of residual stresses. Relaxation of the residual stresses at the surface amounted to around 23% of the residual stresses after SP treatment. No significant changes in

residual-stress measurement of the as-machined and corroded specimens were noticed.

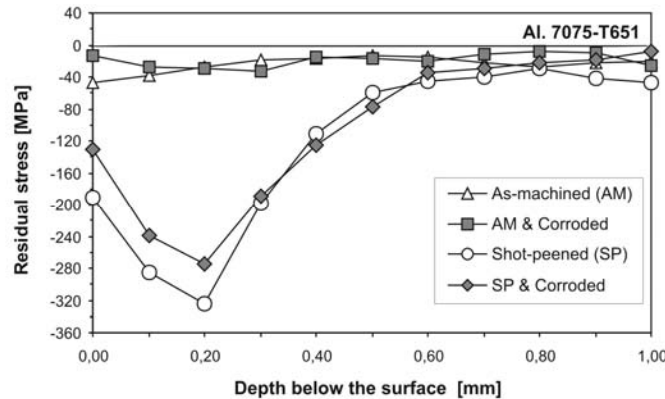


Figure 3. Distribution of residual stresses versus depth for 7075-T651 aluminium.

3.3 Bending Fatigue Testing

The semilogarithmic S-N curves generated for the fatigued specimens in different research combinations are presented in Figure 4. Fatigue results for the as-machined specimens presented a baseline for further comparison of fatigue properties. Because the fatigue tests were limited in number of specimens and applied fatigue load cycles up to 10^7 cycles the more accurate fatigue endurance limit at applied stresses in range of $5 \cdot 10^8$ or even in range of 10^9 cycles can not be confirmed without additional testing. The presence of a corrosive chloride atmosphere has a major influence on materials fatigue properties. Fatigue resistance of the corroded specimens drastically decreased in comparison with the as-machined specimens. Pitting corrosion decrease of fatigue life at individual maximal applied stresses by a factor of about 10 was observed. The fatigue stress limit at 10^7 cycles of corroded specimens with maximal applied stress of 85MPa amounts to only 45% of fatigue stress limit of the as-machined specimens with maximal applied stress of 189MPa. This significant decrease of corroded-specimen fatigue life is contributed to low material resistance to pitting corrosion. Local stress concentrations at pit area contribute to faster fatigue crack initiation.

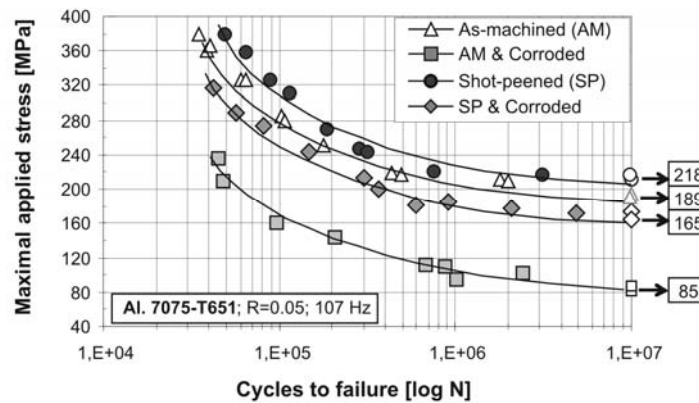


Figure 4. Corrosion fatigue life for 7075-T651 aluminium.

Fatigue testing results indicate a favourable influence of SP treatment on material fatigue resistance. After SP treatment fatigue life improvement increase

nearly by a factor of 2 to as-machined specimens at individual maximal applied fatigue stresses was observed. Further, the SP-treated specimens reached, with regard to the as-machined specimens, the fatigue limit in chosen criterion of 10^7 cycles at 15% higher maximal applied stress. The SP-treated specimens exposed to corrosive chloride environment also showed improved fatigue properties. Fatigue stress limit of the SP-treated and corroded specimens increased to 165MPa at 10^7 cycles. Induced residual compressive stresses retarded fatigue crack initiation in the pit area which resulted in better fatigue properties. Thus fatigue stress limit of the pre-corroded specimens with induced compressive residual stress approached 87% of fatigue stress limit of the as-machined specimens.

3.4 Post Fatigue Fractographic Analysis

In predicting fatigue properties, especially in a corrosive environment, it is important to analyse fatigue crack initiations. To evaluate fatigue crack initiation in the present research, the fractured surfaces on all fatigued specimen were first examined under the optical microscope at low magnification and then cut for further examination at higher magnifications using SEM. Typical SEM images of fracture surfaces of fatigued test specimens are shown in Figure 5.

Fatigue cracks at the tested as-machined specimens and SP-treated specimens initiated at the specimen edges where higher stress concentrations were present. Fatigue crack initiations of the fatigued as-machined samples were found at depths between 50 and 100 μ m below the surface (Fig. 5a). The analysis of the fracture surfaces of the fatigued SP-treated specimens indicated fatigue crack initiation at depths between 150 and 370 μ m below the surface (Fig. 5b). Due to induced residual compressive stresses in the surface layer, fatigue crack initiation was observed at much greater depths with reference to the as-machined specimens. The subsurface fatigue bending stress exceeded the critical fatigue stress below the surface compressive layer so fatigue cracks initiated at much greater depths. Stress concentrations and material deterioration around the pits of the pre-corroded specimens affect the fatigue crack initiation. The critical pit depth of fatigued as-machined and corroded specimens was around 110 μ m at applied stress of 143MPa (Fig. 5c) and around 70 μ m in depth at 101MPa (Fig. 5d). In the SP-treated and corroded specimens fatigued at 172MPa, a fatigue crack initiated from a surface pit at the boundary between two dimples, where a critical pit depth measured 95 μ m (Fig. 5e). An analysis of fractured surface of the SP-treated and corroded specimen fatigued at 185MPa crack initiated at even smaller critical pit depth with around 67 μ m (Fig. 5e).

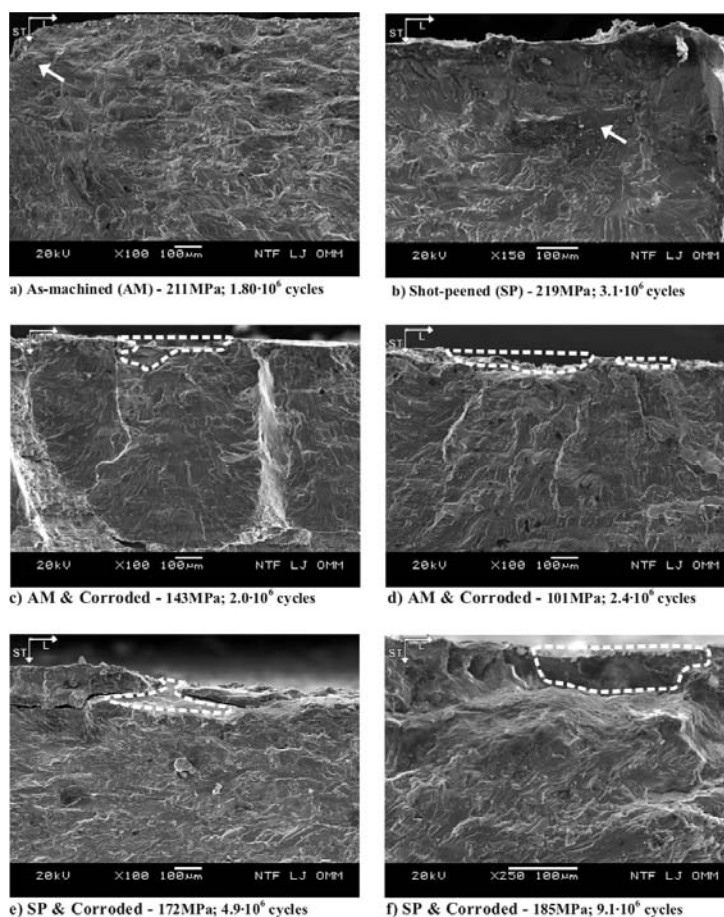


Figure 5. Fractured surface of fatigued specimens. Crack initiation sites are marked with an arrow and critical pits are marked with a dotted line.

3.4 Electrochemical Testing

Electrochemical potentiodynamic testing was conducted to investigate if SP treatment changes the electrochemical characteristics of the material. Based on achieved results prediction of the corrosion rate can be applied and further better interpretation of corrosion fatigue results would be possible. The corrosion potential was determined using potentiodynamic polarisation curves. Results presented in Figure 6 show nearly the same free corrosion potential (E_{corr}) of the as-machined and the SP-treated specimens with values near -700mV . One SP treated specimen had a slightly more positive E_{corr} by about 30mV in reference to an as-machined specimen tested. For comparison of the corrosion current densities (I_{corr}), Tafel analysis was used. The average values of five individual tests for corrosion current densities are given in Table 2. Higher corrosion current density I_{corr} on SP-treated specimens with reference to the as-machined specimens was observed. Increase of corrosion current indicated higher pit growth rate. Electrochemical impedance data show similar corrosion susceptibility indicating that SP-treated material has some lower polarization resistance. The evaluated polarization resistance R_p was $4.3\text{ k}\Omega/\text{cm}^2$ for the as-machined material, while the average value of SP-treated specimens was $3.4\text{ k}\Omega/\text{cm}^2$. The observed detrimental higher corrosion current of the SP-treated material can be compared to the results in.^[18] Increase of I_{corr} by a factor of 5 was reported where specimens were also electrochemically evaluated in

the same direction - the direction of rolling. Induced residual stresses by low plastic burnishing in^[20] showed also the same effect of increasing corrosion current density in the longitudinal (L) direction. But results in the short traverse (ST) directions were in a contrast where the corrosion current density decreased by a factor of about 3.

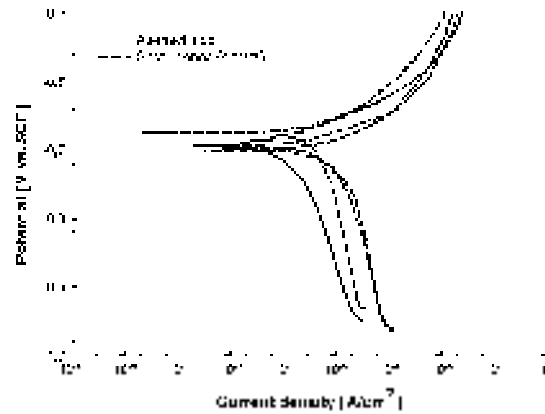


Figure 6. Polarisation curves of as-machined and SP-treated specimens in 0.1M NaCl.

Table 2. Corrosion current densities

Treatment	As-machined	Shot-peened	Ratio
i_{corr} (A/cm ²)	$2.1 \cdot 10^{-6}$	$5.2 \cdot 10^{-6}$	1 : 2.50

In present study of corrosion fatigue resistance the pitting corrosion properties in the rolling direction were important as this direction presented the crack growth direction on fatigued specimens. To estimate the real fatigue life improvement it is important to evaluate the beneficial compressive surface stresses over the depth of critical pits in combination with the possible detrimental higher pit growth rate. Research results showed complex interactions between residual stress distribution, microstructure orientation and grain sizes in different directions. Future work should be planned to combine effects of critical pit-to-crack transition, induced residual stresses and effect of possible changes of pit growth rate of the as-machined base and SP-treated material in all three material microstructural directions L, LT and ST. Development of such probabilistic model to understand these phenomena and finally to predict structural integrity of elements made of high-strength aluminium alloys is under investigation.

4 CONCLUSIONS

To determine the effects of pitting corrosion on fatigue properties of the SP-treated aluminium alloy 7075-T651, a series of tests were performed. The research results demonstrate reasonableness of the SP treatment of structural elements exposed to corrosive chloride environment. Based on the study of the influence of the SP treatment on corrosion fatigue resistance of aluminium alloy 7075-T651 in the 5% NaCl solution fog chamber and in 0.1M NaCl solution, following conclusions can be drawn:

1. Fatigue resistance of the corroded specimens with surface pits drastically decreased in comparison with the as-machined specimens. Decrease of fatigue life at chosen maximal applied stresses by a factor of about 10 was observed. The fatigue stress limit at 10^7 cycles of corroded specimens with maximal applied stress of 85MPa amounts to only 45% of fatigue stress limit of the as-machined specimens

with maximal applied stress of 189MPa. Local stress concentrations at the degraded surface pits area resulted in much faster fatigue crack growth.

2. After the SP treatment the number of surface pits at the evaluated surface was considerably reduced. By SP treatment induced residual compressive stresses retarded fatigue crack initiation in the pit area which resulted in better specimen fatigue properties in corrosive environment nearly by factor of 2.

3. In electrochemical potentiodynamic testing higher corrosion current density on the SP-treated specimens with reference to the as-machined material was observed. Increase of corrosion current indicated higher pit growth rate.

4. To estimate the real fatigue life improvement it is important to evaluate the beneficial compressive surface stresses over the depth of critical pits in combination with the detrimental higher corrosion current density observed in rolling direction of tested material.

REFERENCES

- 1 Vargel C. (Schmidt MP), 2004. Corrosion of aluminum. Oxford (UK): Elsevier Ltd., pp. 142-144.
- 2 Pao, P.S., Gill, S.J., Feng, C.R., 2000. On fatigue crack initiation from corrosion pits in 7075-T7351 aluminum alloy. *Scripta Mater.* 43, 391-396.
- 3 Genel, K., 2007. The effect of pitting on the bending fatigue performance of high-strength aluminum alloy. *Scripta Mater.* 57, 297-300.
- 4 Wang, Q.Y., Kawagoishi, N., Chen, Q., 2003. Effect of pitting corrosion on very high cycle fatigue behavior. *Scripta Mater.* 49, 711-716.
- 5 DuQuesnay, D.L., Underhill, P.R., Britt, H.J., 2003. Fatigue crack growth from corrosion damage in 7075-T6511 aluminum alloy under aircraft loading. *Int. J. Fatigue* 25, 371-377.
- 6 Jones, K., Hoepfner, D.W., 2005. Pit-to-crack transition in pre-corroded 7075-T6 aluminum alloy under cyclic loading. *Corr. Sci.* 47, 2185-2198.
- 7 Sankaran, K.K., Perez, R., Jata, K.V., 2001. Effect of pitting corrosion on the fatigue behavior of aluminum alloy 7075-T6: modeling and experimental studies. *Mat. Sci. and Eng. A297*, 223-229.
- 8 Pidaparti, R.M., Patel, R.R., 2008. Correlation between corrosion pits and stresses in Al alloys. *Materials Letters* 62, 4497-4499.
- 9 Sharp, P.K., Clark, G., 2001. The effect of peening on the fatigue life of 7050 aluminium alloy. *Reserch Report DSTO-RR-0208*. Accessed at: <http://hdl.handle.net/1947/3292>.
- 10 Shen, S., Han, Z.H., Herrera, C.A., Atluri, S.N., 2004. Assessment, development, and validation of computational fracture mechanics methodologies and tools for shot-peened materials. *Final Report. DOT/FAA/AR-03/76*.
- 11 Rodopoulos, C.A., Curtis, S.A, Rios, E.R., SolisRomero, J., 2004. Optimization of the fatigue resistance of 2024-T351 aluminium alloys by controlled shot peening-methodology, results and analysis. *Int. J. Fatigue* 26, 849-856.
- 12 Benedetti, M., Fontanari, V., Scardi, P., Ricardo, C.L.A., Bandini, M., Reverse bending fatigue of shot peened 7075-T651 aluminium alloy. *Int. J. Fatigue.* 31, 1225-1236.
- 13 George, P.M., Pillai, N. and Shah, N. 2004. Optimization of shot peening parameters using Taguchi technique. *Mat. Proc. Techn. Vol. 153-154*, pp. 925-930.
- 14 Guagliano, M. 2001. Relating Almen intensity to residual stresses induced by shot peening: a numerical approach. *Mat. Proc. Techn. Vol. 110*, pp. 277-286.
- 15 ASTM B117-07a Standard Practice for Operating Salt Spray (Fog) Apparatus.
- 16 ASTM E837-08 Standard Test Method for Determining Residual Stresses by the Hole-Drilling Strain-Gage Method.

- 17 Li, J.K., Mei, Y., Wang, D., and Wang, R. 1992. An analysis of stress concentration caused by shot peening and its application in predicting fatigue strength. *Fatigue Fract. Eng. Mater Struct.* Vol. 152, 1271-1279.
- 18 Curtis, S.A., Rios, E.R., Rodopoulos, C.A., Romero, J.S., Levers, A. 2003. Investigating the Benefits of Controlled Shot Peening on Corrosion Fatigue of Aluminium Alloy 2024 T351. In: *Proceedings of 8th Int. Conf. on Shot Peening (ICSP-8)*, Garmish-Partenkirchen, Germany, pp.16-20.
- 19 Prevey, P.S., Cammett, J.T., 2004. The influence of surface enhancement by low plasticity burnishing on the corrosion fatigue performance of AA7075-T6. *Int. J. Fatigue* 26, 975-982.
- 20 Liu, X., Frankel, G.S. 2006. Effect of compressive stress on localized corrosion in AA2024-T3. *Corr. Sci.* 48, 3309-3329.